Journal of Molecular Liquids 349 (2022) 118172

Contents lists available at ScienceDirect

Journal of Molecular Liquids

journal homepage: www.elsevier.com/locate/molliq

Thermodynamic study and preferential solvation of sulfamerazine in acetonitrile + methanol cosolvent mixtures at different temperatures

Rossember E. Cárdenas-Torres [a], Claudia Patricia Ortiz [b], William E. Acree Jr [c], Abolghasem Jouyban [d,e], Fleming Martínez [f], Daniel Ricardo Delgado [g,*]

[a] Grupo de Fisicoquímica y Análisis Matemático, Facultad de Ciencias y Humanidades, Fundación Universidad de América, Avda Circunvalar No. 20-53, Bogotá D. C., Colombia
[b] Corporación Universitaria Minuto de Dios-UNIMINUTO, Programa de Administración en Seguridad y Salud en el Trabajo, Grupo de Investigación en Seguridad y Salud en el Trabajo, Neiva, Colombia
[c] Department of Chemistry, University of North Texas, Denton, TX 76203-5070, USA
[d] Pharmaceutical Analysis Research Center and Faculty of Pharmacy, Tabriz University of Medical Sciences, Tabriz, Iran
[e] Faculty of Pharmacy, Near East University, 99138 Nicosia, North Cyprus, Mersin 10, Turkey
[f] Universidad Nacional de Colombia, Sede Bogotá, Facultad de Ciencias, Departamento de Farmacia, Grupo de Investigaciones Farmacéutico-Fisicoquímicas, Carrera 30 No. 45-03, Bogotá D.C., Colombia
[g] Universidad Cooperativa de Colombia, Facultad de Ingeniería, Programa de Ingeniería Civil, Grupo de Investigación de Ingenierías UCC-Neiva, Calle 11 No. 1- 51, Neiva, Huila, Colombia

ARTICLE INFO

Article history:
Received 28 July 2021
Revised 21 October 2021
Accepted 20 November 2021
Available online 28 November 2021

Keywords:
Sulfamerazine
{Acetonitrile (1) + methanol (2)} mixtures
Dissolution thermodynamics
Preferential solvation
IKBI
Mathematical model

ABSTRACT

This paper discusses sulfamerazine (SMR) solubility in Acetonitrile (MeCN) + Methanol (MeOH) cosolvents at nine temperatures (278.15–318.15 K). Herein, the maximum SMR solubility was reached in a cosolvent mixture at the highest studied temperature, and the minimum SMR solubility was reached in neat methanol at the lowest studied temperature. Using experimental data, thermodynamic functions were calculated for both the solution and mixture using the Gibbs and van't Hoff equations, thus determining that the solution process is endothermic with entropic favoring. In addition, the preferential solvation parameters ($\delta x_{3,1}$), calculated using the inverse Kirkwood-Buff integrals (IKBI) method, are reported; SMR is preferentially solvated by MeOH in MeOH-rich mixtures, and in intermediate and MeCN-rich mixtures, the $\delta x_{3,1}$ values indicate that SMR is not preferentially solvated by any of the two solvents in the mixture (MeCN + MeOH). Finally, eight models were assessed (Apelblat, van't Hoff, Yaws, λh, Weibull, NRTL, Wilson, and Wilson modified), with all presenting mean relative deviation percentages (MRD%) under 6%, which indicates a good correlation with the experimental data.

1. Introduction

Sulfamerazine, (SMR) (4-amino-*N*-(4-methylpyrimidin-2-yl) benzenesulfonamide; CAS: 127-79-7) (Fig. 1) is a long-acting antibacterial agent, which inhibits the dihydrofolic acid synthesis ((2S)-2-[[4-[(2-amino-4-oxo-7,8-dihydro-3*H*-pteridin-6-yl) methylamino] benzoyl] amino] pentanedioic acid) by competing with the *para*-aminobenzoic acid by the dihydropteroate synthase binding site [1].

In combination with trimethoprim, sulfamerazine is used in the treatment of opportunistic infections related to AIDS, urinary tract infections, bronchitis, infections caused by Escherichia coli, bacterial eye infections, among others [1], and it is widely used for treating infections in animals [2]. SMR is also used as a food preservative because of its great antibacterial potential [3].

The increased use of sulfamerazine has led entities, such as the NORMAN network, to classify it as an emerging pollutant. In other words, sulfamerazine is considered as an environmental problem that must be addressed. In addition, countries such as Mexico, USA, China, and countries of the European Union have established permissible limits for sulfonamides in animal meat for human consumption [4].

The massive use of this drug has also led to the development of a large number of solubility studies, focusing on pure solvents and cosolvent mixtures, due to its importance in formulation, purification, stability, recrystallization, and other specific pharmaceutical industry processes [5].

Delgado et al. assessed SMT solubility behavior in different cosolvent mixtures at different temperatures. Some of these mixtures are: methanol + water [6], ethanol + water [7],

* Corresponding author.
E-mail address: danielr.delgado@campusucc.edu.co (D.R. Delgado).

https://doi.org/10.1016/j.molliq.2021.118172
0167-7322/

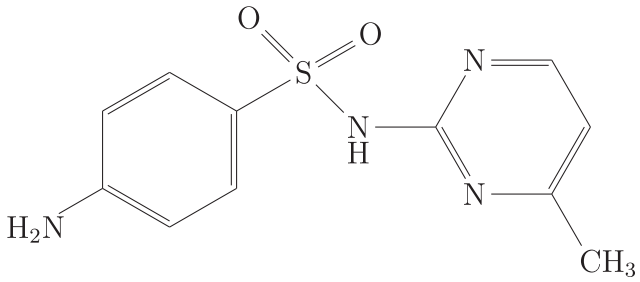

Fig. 1. Sulfamerazine chemical formula.

n-propanol + water [8], and acetonitrile + water [9]. Muños et al. studied the drug's solubility in propylene glycol + water cosolvent mixtures [10], and Aloisio et al. developed solubility studies using cyclodextrins and meglumine [11].

Regarding the solvents used in this study, they are widely used in the chemical and pharmaceutical industries for many of its processes, especially in drug quantification using high pressure liquid chromatography (HPLC), in addition to other practices, such as recrystallization and microencapsulation [12–14].

Regarding solubility studies of cosolvents in this system, Zhang et al. reported the solubility of Dibenzothiophene [15] and Delgado et al. studied sulfadiazine at different temperatures [16].

In this context, the main objective of this research is to assess the cosolvent effect from the Acetonitrile (MeCN) + Methanol (MeOH) mixture on SMR solubility and perform a thermodynamic and preferential solvation analysis.

2. Experimental section

2.1. Materials and reagents

In this study, SMR (Sigma-Aldrich, USA; compound 3, purity at least 0.990 in mass fraction), MeCN (Merck A.R., Germany; solvent component 1, purity at least 0.990 in mass fraction), and MeOH (Merck A.R., Germany; solvent component 2, purity at least 0.990 in mass fraction), were used. Chemical suppliers, purities, and other select properties of the reagents are summarized in Table 1.

2.2. Preparation of solvent mixtures

All {MeCN (1) + MeOH (2)} solvent mixtures were prepared by mass, using a (RADWAG AS 220.R2, Poland) analytical balance with sensitivity ± 0.1 mg, in quantities of 50.00 g. The mass fractions of MeCN of the nine mixtures prepared, varied by 0.05 from w_1 = 0.05 to w_1 = 0.95.

2.3. Solubility determinations

SMT solubility was determined using the shake-bottle method, quantifying the drug by UV/Vis spectrophotometry. For these purposes, in a 10-ml amber bottle, SMR was added to 10 g of cosolvent mixture until part of the SMT does not dissolve, forming a solid phase at the bottom of the bottle. This factor guarantees that the liquid phase of the bottle corresponds to a saturated solution. Subsequently, the flasks were transferred to refrigeration thermostats (Medingen K-22/T100, Germany), initially at 318.15 K for 48 h, with periodic shaking. Once equilibrium is attained (concentration of the solution remains constant), a sample is taken from each flask and filtered under isothermal conditions through a 0.45-μm membrane (Millipore Corp. Swinnex®-13, USA). Then, it is subsequently diluted with a 0.01 N NaOH solution (to avoid precipitation of the SMR) and the absorbance of the sample is measured at 268 nm (UV/VIS EMC-11-UV spectrophotometer, Germany). All experiments were performed three times. The previous procedure was repeated at each temperature studied; in other words, the procedure was repeated from 318.15 K to 278.15 K, decreasing at 5-degree intervals (9 different temperatures)

2.4. Solid phase DSC analysis

To identify the nature of the SMR bottom solid phases in equilibrium with the saturated solutions in both neat MeCN and MeOH solvents and the mixture w_1 = 0.50 some DSC analyses were performed (DSC 204 F1 Phoenix, Germany). Nearly 5.0 mg of SMR sample was analyzed. The equipment was calibrated using Indium as standard. The sample and reference pans were heated to preserve the programmed temperature at a precise heating rate of 10 $K \cdot min^{-1}$ in a dynamic nitrogen atmosphere (10 $cm^3 \cdot min^{-1}$) at constant pressure.

3. Results and discussion

3.1. Experimental mole fraction solubility

SMR experimental solubility, in (MeCN + MeOH) cosolvent mixtures expressed in molar fraction, is presented in Table 2. The solubility data in pure methanol and in pure acetonitrile were taken from the literature reported by our research group [6,9].

Fig. 2 illustrates SMR solubility behavior as a function of the MeCN mass fraction in the cosolvent mixture (top) and the Hildebrand solubility parameter (bottom). For a binary mixture δ_{1+2} can be calculated by means of $\delta_{1+2} = f_1 \cdot \delta_1 + (1-f_1) \cdot \delta_2$ from the Hildebrand solubility parameter of the neat solvents {δ_1 = 24.1 $MPa^{1/2}$ for ACN (1) and δ_2 = 29.6 $MPa^{1/2}$ for methanol (2)}[17,18]. In all cases, solubility increases at the same time as the temperature, thus indicating an endothermic process. Herein, lowest solubility was reached in pure methanol (δ = 29.6 $MPa^{1/2}$) at 278.15 K and highest was reached in the cosolvent mixture w_1 = 0.40 (δ = 27.4 $MPa^{1/2}$) at 318.15 K. In general terms, all isotherms peak between w_1 = 0.35 (δ = 27.7 $MPa^{1/2}$) and w_1 = 0.40 (δ = 27.4 $MPa^{1/2}$) for mixtures with a solubility parameter similar to SMR (28.10 $MPa^{1/2}$). This behavior is remarkably similar to sulfadiazine (28.89 $MPa^{1/2}$) in the same cosolvent mixture, where the maximum solubility in each solubility isotherm was reached at w_1 = 0.25 (δ = 28.2 $MPa^{1/2}$) and w_1 = 0.30 (δ = 27.9 $MPa^{1/2}$). The maximum solubility Sulfadiazine (SD) isotherm peaks are presented in cosolvent mixtures with solubility parameters higher than SMR, demonstrating the influence

Table 1
Source and purities of the compounds used in this research.

Compound	CAS	Formula	Molar mass g mol^{-1}	Source	Purity in mass fraction	Analytic technique [a]
Sulfamerazine	127–79-7	$C_{11}H_{12}N_4O_2S$	264.30	Sigma-Aldrich, USA	>0.99	HPLC
Methanol	67–56-1	CH_4O	32.04	Merck A.R., Germany	>0.99	GC
Acetonitrile	75–05-8	C_2H_3N	41.05	Merck A.R., Germany	>0.99	GC

[a] HPLC is high liquid performance chromatography, GC is gas chromatography.

Table 2
Experimental mole fraction solubility ($10^3\ x_3$) of sulfamerazine in {acetonitrile (1) + methanol (2)} mixtures at several temperatures.

w_1 [a,b]	T/K [b]								
	278.15	283.15	288.15	293.15	298.15	303.15	308.15	313.15	318.15
0.00	0.461	0.535	0.623	0.767	0.870	1.04	1.17	1.35	1.49
0.05	0.541	0.661	0.799	1.01	1.16	1.40	1.68	1.97	2.25
0.10	0.700	0.859	1.06	1.31	1.60	1.92	2.30	2.73	3.20
0.15	0.853	1.07	1.33	1.70	2.03	2.51	3.00	3.62	4.55
0.20	1.03	1.27	1.60	2.04	2.46	3.06	3.63	4.43	5.70
0.25	1.21	1.55	1.98	2.46	2.92	3.71	4.55	5.50	6.72
0.30	1.46	1.85	2.35	2.87	3.54	4.34	5.24	6.51	7.58
0.35	1.52	1.90	2.45	3.03	3.69	4.55	5.39	6.70	7.92
0.40	1.53	1.93	2.43	3.01	3.68	4.45	5.34	6.61	7.94
0.45	1.50	1.92	2.38	2.92	3.60	4.29	5.30	6.49	7.81
0.50	1.50	1.86	2.31	2.81	3.47	4.22	5.11	6.34	7.66
0.55	1.48	1.83	2.28	2.73	3.39	4.10	4.96	6.06	7.35
0.60	1.46	1.81	2.22	2.69	3.29	4.02	4.75	5.89	7.12
0.65	1.43	1.77	2.17	2.60	3.21	3.89	4.60	5.67	6.92
0.70	1.40	1.75	2.11	2.55	3.10	3.79	4.54	5.50	6.74
0.75	1.39	1.71	2.07	2.50	2.95	3.62	4.35	5.38	6.47
0.80	1.37	1.68	2.00	2.42	2.80	3.45	4.25	5.20	6.33
0.85	1.35	1.64	1.95	2.37	2.71	3.29	4.14	5.06	6.14
0.90	1.33	1.62	1.90	2.26	2.66	3.15	3.91	4.88	6.00
0.95	1.32	1.57	1.84	2.18	2.52	3.05	3.77	4.65	5.88
1.00	1.31	1.51	1.74	2.01	2.29	2.71	3.47	4.32	5.72
Ideal	2.77	3.29	3.91	4.62	5.45	6.41	7.53	8.81	10.28

[a] w_1 is the mass fraction of acetonitrile (1) in the {acetonitrile (1) + methanol (2)} mixtures free of sulfamerazine (3).
[b] Average relative standard uncertainty in w_1 is $u_r(w_1) = 0.0008$. Standard uncertainty in T is $u(T) = 0.10$ K. Average relative standard uncertainties in x_3 is $u_r(x_{3(1+2)}) = 0.019$.

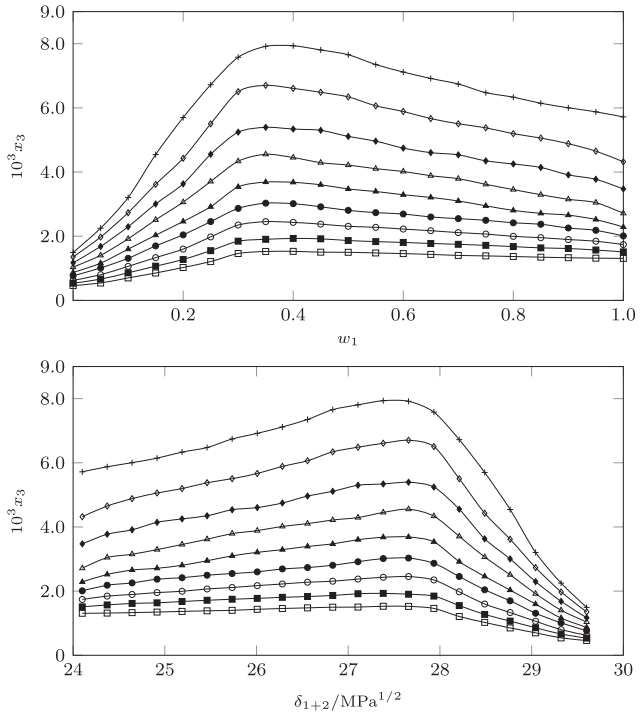

Fig. 2. Sulfamerazine mole fraction solubility (x_3) as a function of the mass fraction of acetonitrile (top) and Hildebrand solubility parameter (bottom) of the {acetonitrile (1) + methanol (2)} mixtures at different temperatures. □: 278.15 K; ■: 283.15 K; ○: 288.15 K; ●: 293.15 K; ▲: 298.15 K; Δ: 303.15 K; ◆: 308.15 K; ◇: 313.15 K; +: 318.15 K.

of the SMR $-CH_3$ group, which makes SMR polarity less than the one of SD [16]. However, SD solubility is lower than SMR solubility. This is possibly due to the fact that solute–solute interactions are less energetic for SMR, especially because SD fusion enthalpy (44.3 kJ·mol^{-1}) is greater than SMR fusion enthalpy (41.3 kJ·mol^{-1}) [17]. Therefore, we can conclude that SMR solubility is strongly influenced by the cosolvent system polarity.

Now, in MeOH-rich mixtures, SMR could form hydrogen bonds between the —OH group of MeOH and its —NH_2, —SO_2—, and =N- groups, acting as a Lewis base and the —NH_2 and ≥N—H groups acting as a Lewis acid. When MeCN concentrations increase, which is a mid-polarity aprotic solvent, SMR solubility increases, possibly due to the fact that nonpolar interactions also increase, reaching their maximum solubility in a cosolvent mixture with a solubility parameter similar to the one presented by the drug.

3.2. Solid phases DSC analysis

DSC thermograms of SMR bottom solid phases in equilibrium with the saturated solutions in both neat solvents MeCN and MeOH and the mixture w_1 = 0.50 are depicted in Fig. 3. As can be seen, in all cases there is an endothermic peak corresponding to the melting of SMR. Observed on-set temperature of melting was MeCN = 507.4 K, $w_{0.5}$ = 509.1 K and MeOH = 508.8 K, which is almost coincident with the reported value for original sample 508.5 K [7,19]. From this, it is evident that no polymorphic transformations or solvate formations were observed.

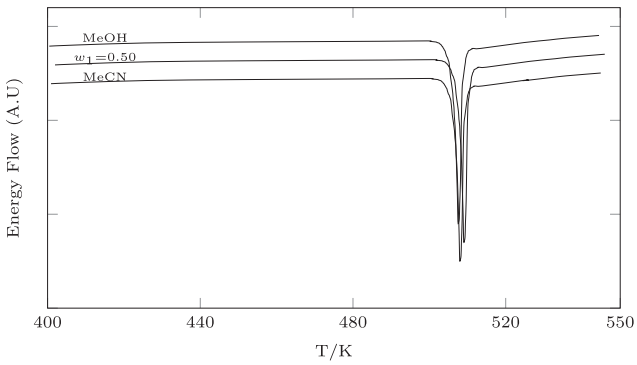

Fig. 3. DSC thermograms of sulfamerazine as bottom phases in equilibrium with saturated solutions. Acetonitrile; {acetonitrile (1) + methanol (2)}, w_1 = 0.5; methanol.

3.3. Activity coefficients in mixed solvents

In Table 3, SMR activity coefficients in (MeCN + MeOH) cosolvent mixtures calculated according to Eq. (1) are presented.

$$\gamma_3 = \frac{e^{\left\{-\frac{\Delta_{fus}H(T_{fus}-T)}{RT_{fus}T}+\frac{\Delta C_p}{R}\left[\frac{T_{fus}-T}{T}+\ln\left(\frac{T_{fus}}{T}\right)\right]\right\}}}{x_3} \quad (1)$$

where $\Delta_{fus}H$ is the molar enthalpy of fusion of the pure solute, T_{fus} is the absolute melting point, T is the absolute solution temperature, R is the gas constant (8.3145 J·mol^{-1}·K^{-1}), and ΔC_p is the difference between the molar heat capacity of the SMR crystalline form and the molar heat capacity of the hypothetical supercooled liquid form, both at the solution temperature. The enthalpy of fusion and the melting temperature were determined experimentally using DSC, the data were reported in previous works developed by the research group (T_{fus} = 508.5 K and $\Delta_{fus}H$ = 41.3 ± 0.7 kJ·mol^{-1}) [7]; since ΔC_p cannot be easy experimentally determined it is usual assuming that it may be approximated to the entropy of fusion, $\Delta_{fus}S$ calculated as the quotient $\Delta_{fus}H/T_{fus}$, *i.e.* 81.2 ± 0.7 J·mol^{-1}·K^{-1} [19].

In all cases, SMR activity coefficients are >1, indicating that the experimental solubility is lower than the ideal solubility.

However, it should be noted that in all cases values are between 1.3 and 6.88, indicating a quasi-ideal global process compared to the values obtained for the same drug in water-rich systems, wherein activity coefficient values reached up to 10 times higher [6].

Comparing SD and SMR in the same cosolvent system, SMR exhibits activity coefficients values closer to ideal (1.0) [16].

From Eq. (2), which expresses the activity coefficient as a function of the possible molecular interactions solute–solute (e_{33}), solvent–solute (e_{s3}), and solvent–solvent (e_{ss}), an approximate estimate of the magnitude of these iterations may be calculated.

$$\ln\gamma_3 = (e_{ss} + e_{33} - 2e_{s3})\frac{V_3\phi_s^2}{RT} \quad (2)$$

Hence, the solute–solute (e_{33}) and solvent–solvent (e_{ss}) molecular interactions would be higher in pure methanol (δ = 29.6 MPa$^{1/2}$), a solvent which reports the highest γ_3 (6.88) values. When adding MeCN to the system between w_1 = 0.0 and w_1 = 0.35/0.40, the γ_3 values decrease, favoring solute–solvent iterations (e_{13}), which are consistent with the increase in SMT solubility. From w_1 = 0.35/0.40 (δ = 34.71/35.12 MPa$^{1/2}$) to pure MeCN (δ = 24.1 MPa$^{1/2}$), γ_3 values denote an increase again, indicating a disadvantage for solute–solvent iterations (e_{s3}). In all cases, solute–solute (e_{33}) and solvent–solvent (e_{ss}) internments, which do not favor SMR solubility, are greater than solute–solvent interactions (e_{s3}), which favor SMR solubility.

3.4. Apparent thermodynamic functions of dissolution

Table 4 lists the solution thermodynamic functions, calculated using the Gibbs and van't-Hoff-Krug approach based on experimental solubility data (Table 2).

$$\left(\frac{\partial \ln x_3}{\partial(1/T - 1/T_{hm})}\right)_p = -\frac{\Delta_{soln}H^\circ}{R} \quad (3)$$

$$\Delta_{sonl}G^o = -RTa \quad (4)$$

$$\Delta_{soln}S^o = \frac{(\Delta_{soln}H^\circ - \Delta_{soln}G^\circ)}{T_{hm}} \quad (5)$$

$$\zeta_H = \frac{|\Delta_{soln}H^\circ|}{|\Delta_{soln}H^\circ| + |T\Delta_{soln}S^\circ|} \quad (6)$$

$$\zeta_{TS} = \frac{|T\Delta_{soln}S^\circ|}{|\Delta_{soln}H^\circ| + |T\Delta_{soln}S^\circ|} \quad (7)$$

where, $\Delta_{soln}H^\circ$, $\Delta_{soln}G^\circ$, and $\Delta_{soln}S^\circ$ are the enthalpy, Gibbs energy, and standard entropy of the solution, respectively (kJ·mol^{-1}); T is the study temperature (K); T_{hm} is the harmonic mean of the study temperatures (K); R is the universal constant of ideal gases (8.3145 J·mol^{-1}·K^{-1}); a is the intercept of the van't-Hoff-Krug equation (Fig. 4) (ln x_3); ζ_H and ζ_{TS} are the fractional contribution of the enthalpic and entropic terms, respectively.

The harmonic temperature ($T_{hm} = n/\sum 1/T$) used in this study is 297.59 K. When plotting ln x_3 vs. $T^{-1} - T_{hm}^{-1}$, (as shown in Fig. 4 for some solvent systems) the slope and intercept data necessary for

Table 3
Activity coefficients of sulfamerazine in {acetonitrile (1) + methanol (2)} mixtures at several temperatures.

w_1 [a]	T/K [b]								
	278.15	283.15	288.15	293.15	298.15	303.15	308.15	313.15	318.15
0.00	6.01	6.15	6.27	6.03	6.27	6.19	6.43	6.51	6.88
0.05	5.11	4.98	4.89	4.58	4.70	4.57	4.48	4.46	4.57
0.10	3.96	3.84	3.69	3.53	3.42	3.34	3.28	3.22	3.21
0.15	3.25	3.09	2.93	2.72	2.68	2.55	2.50	2.43	2.26
0.20	2.70	2.59	2.45	2.26	2.22	2.10	2.07	1.99	1.80
0.25	2.29	2.13	1.98	1.88	1.87	1.73	1.65	1.60	1.53
0.30	1.90	1.79	1.66	1.61	1.54	1.48	1.44	1.35	1.36
0.35	1.82	1.73	1.59	1.53	1.48	1.41	1.40	1.31	1.30
0.40	1.81	1.71	1.61	1.53	1.48	1.44	1.41	1.33	1.30
0.45	1.84	1.72	1.64	1.59	1.51	1.49	1.42	1.36	1.32
0.50	1.85	1.77	1.69	1.65	1.57	1.52	1.47	1.39	1.34
0.55	1.87	1.80	1.72	1.69	1.61	1.56	1.52	1.45	1.40
0.60	1.90	1.82	1.76	1.72	1.66	1.60	1.59	1.50	1.44
0.65	1.93	1.86	1.80	1.78	1.70	1.65	1.63	1.55	1.49
0.70	1.98	1.89	1.85	1.81	1.76	1.69	1.66	1.60	1.52
0.75	2.00	1.92	1.89	1.85	1.85	1.77	1.73	1.64	1.59
0.80	2.02	1.97	1.96	1.91	1.94	1.86	1.77	1.69	1.62
0.85	2.06	2.01	2.00	1.95	2.01	1.95	1.82	1.74	1.67
0.90	2.08	2.04	2.06	2.05	2.05	2.04	1.92	1.80	1.71
0.95	2.10	2.10	2.12	2.12	2.16	2.11	1.99	1.89	1.75
1.00	2.11	2.18	2.25	2.30	2.39	2.36	2.17	2.04	1.80

[a] x_1 is the mass fraction of acetonitrile (1) in the {acetonitrile (1) + methanol (2)} mixtures free of sulfamerazine (3).
[b] Average relative standard uncertainty in w_1 is $u_r(w_1)$ = 0.0008. Standard uncertainty in T is $u(T)$ = 0.10 K. Average relative uncertainty in γ_3 is $u_r(\gamma_3)$ = 0.021.

Table 4
Apparent thermodynamic functions relative to dissolution processes of sulfamerazine (3) in {acetonitrile (1) + methanol (2)} mixtures at T_{hm} = 297.6 K.

w_1 [a,b]	$\Delta_{soln}G°$/kJ mol^{-1} [b]	$\Delta_{soln}H°$/kJ mol^{-1} [b]	$\Delta_{soln}S°$/J mol^{-1} K^{-1} [b]	$T\Delta_{soln}S°$/kJ mol^{-1} [b]	ζ_H [c]	ζ_{TS} [c]
0.00	17.47	22.23	16.00	4.76	0.824	0.176
0.05	16.75	26.52	32.84	9.77	0.731	0.269
0.10	16.01	28.21	40.99	12.20	0.698	0.302
0.15	15.37	30.39	50.45	15.01	0.669	0.331
0.20	14.90	31.03	54.22	16.13	0.658	0.342
0.25	14.42	31.28	56.67	16.86	0.650	0.350
0.30	14.02	30.42	55.11	16.40	0.650	0.350
0.35	13.92	30.33	55.16	16.42	0.649	0.351
0.40	13.93	30.07	54.23	16.14	0.651	0.349
0.45	13.98	30.03	53.95	16.06	0.652	0.348
0.50	14.04	29.91	53.32	15.87	0.653	0.347
0.55	14.11	29.37	51.29	15.26	0.658	0.342
0.60	14.17	28.96	49.69	14.79	0.662	0.338
0.65	14.24	28.66	48.47	14.43	0.665	0.335
0.70	14.30	28.58	48.01	14.29	0.667	0.333
0.75	14.37	28.07	46.04	13.70	0.672	0.328
0.80	14.45	27.92	45.25	13.47	0.675	0.325
0.85	14.52	27.65	44.13	13.13	0.678	0.322
0.90	14.59	27.24	42.48	12.64	0.683	0.317
0.95	14.67	26.94	41.20	12.26	0.687	0.313
1.00	14.83	26.18	38.13	11.35	0.698	0.302
Ideal	12.92	24.13	37.67	11.21	0.683	0.317

[a] x_1 is the mass fraction of acetonitrile (1) in the {acetonitrile (1) + methanol (2)} mixtures free of sulfamerazine (3).
[b] Average relative standard uncertainty in w_1 is $u_r(w_1)$ = 0.0008. Standard uncertainty in T is $u(T)$ = 0.10 K. Average relative standard uncertainty in apparent thermodynamic quantities of real dissolution processes are $u_r(\Delta_{soln}G°)$ = 0.020, $u_r(\Delta_{soln}H°)$ = 0.024, $u_r(\Delta_{soln}S°)$ = 0.031, $u_r(T\Delta_{soln}S°)$ = 0.031.
[c] ζ_H and ζ_{TS} are the relative contributions by enthalpy and entropy toward apparent Gibbs energy of dissolution.

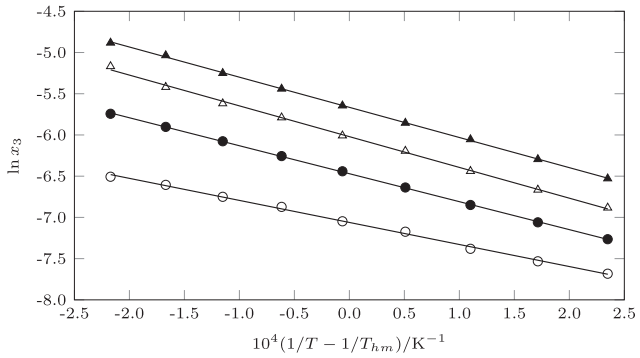

Fig. 4. van't Hoff plot of the solubility of sulfamerazine (3) in some {acetonitrile (1) + methanol (2)} mixtures. ○: neat acetonitrile, ●: w_1 = 0.10, Δ: w_1 = 0.20, ▲: w_1 = 0.20.

the calculation of the enthalpy and Gibbs energy of solution are obtained.

Hence, the solution Gibbs energy is positive. In all cases, it decreases from pure MeOH to the cosolvent mixture w_1 = 0.35, where maximum SMR solubility is reached. From this cosolvent mixture to pure MeCN, the Gibbs energy value increases due to the decrease in solubility as a consequence of the increase in MeCN concentration, which decreases the polarity of the solvent medium and drives it further from SMR polarity (28.10 MPa$^{1/2}$).

As for the solution standard enthalpy, it is positive in all cases. This indicates an endothermic process, which would at first be an unfavorable factor for the solution process. The behavior of the enthalpy of the solution is similar to the behavior of SMR in some aqueous solutions [6]. From the most polar medium (pure MeOH (δ = 29.6 MPa$^{1/2}$)) to w_1 = 0.25, the standard enthalpy of the solution increases as it usually occurs in aqueous media due to water destructuring. However, in this case, the most polar medium is pure MeOH. Pierce and MacMillan [20] have demonstrated the association of alcohol molecules, which is greater in low molar mass alcohols. Therefore, as MeCN concentration increases, these MeOH-MeOH agglomerations decrease, breaking the MeOH-MeOH bond. In fact, this could explain the initial behavior exhibited by the enthalpy of the solution; from w_1 = 0.25 until pure MeCN the standard enthalpy of solution decreases.

As for the standard entropy of the solution, it is positive in all cases, which favors the solution process. Finally, according to Eqs. (6) and (7), the enthalpy of the solution is the largest contributor to the Gibbs energy value of the solution, reporting values of 64.9% and 82.4 %.

3.5. Apparent thermodynamic quantities of mixing

Hypothetically the solution process can be represented in four stages:

$$\text{Solute}_{(\text{Solid})} \text{ at } T_i \rightarrow \text{Solute}_{(\text{Solid})} \text{ at } T_{fus} \rightarrow \text{Solute}_{(\text{Liquid})} \text{ at } T_{fus} \rightarrow Solute_{(\text{Liquid})} at T_i \rightarrow Solute_{(\text{Solution})} at T_i$$

The first stage consists heating the solute in solid state from a temperature of T_i to the solute melting temperature. The second stage consists changing its state from solid to liquid under isothermal conditions. In the third stage, the solute temperature in the liquid state decreases its temperature to T_i. Finally, in the fourth stage, the solute and solvent, both in the liquid state at T_i, interact to form the solution. In this particular case, $T_i = T_{hm}$ = 297.6 K.

The thermodynamic functions of the previous process can be expressed mathematically as:

$$\Delta_{soln}H^{\circ} = \Delta_{soln}H^{\circ-id} + \Delta_{mix}H^{\circ} \quad (8)$$

$$\Delta_{soln}S^{o} = \Delta_{soln}S^{o-id} + \Delta_{mix}S^{o}. \quad (9)$$

In Eqs. (8) and (9), the fusion thermodynamic functions are replaced by the ideal solution thermodynamic functions (Table 4). Hence, in Table 5, the thermodynamic functions for the SMR mixture in (MeCN + MeOH) cosolvent mixtures are presented. The Gibbs energy of the mixture is positive in all cases, indicating a disadvantage of the mixing process for the overall solution process. Regarding the enthalpy of the mixture, it increases from pure MeOH up to w_1 = 0.25 and decreases from this MeCN mass fraction to pure MeCN. Although the enthalpy corresponding to the cavity formation

Table 5
Apparent thermodynamic functions relative to mixing processes of sulfamerazine (3) in {acetonitrile (1) + methanol (2)} mixtures at T_{hm} = 297.6 K.

w_1 [a,b]	$\Delta_{mix}G°$/kJ mol^{-1} [b]	$\Delta_{mix}H°$/kJ mol^{-1} [b]	$\Delta_{mix}S°$/J mol^{-1} K^{-1} [b]	$T\Delta_{mix}S°$/kJ mol^{-1} [b]	ζ_H [c]	ζ_{TS} [c]
0.00	4.55	−1.89	−21.66	−6.45	0.227	0.773
0.05	3.83	2.39	−4.82	−1.44	0.625	0.375
0.10	3.09	4.08	3.32	0.99	0.805	0.195
0.15	2.46	6.26	12.78	3.80	0.622	0.378
0.20	1.98	6.90	16.55	4.93	0.584	0.416
0.25	1.50	7.16	19.00	5.66	0.559	0.441
0.30	1.10	6.29	17.44	5.19	0.548	0.452
0.35	1.00	6.21	17.50	5.21	0.544	0.456
0.40	1.01	5.94	16.57	4.93	0.547	0.453
0.45	1.06	5.91	16.29	4.85	0.549	0.451
0.50	1.12	5.78	15.66	4.66	0.554	0.446
0.55	1.19	5.24	13.62	4.05	0.564	0.436
0.60	1.25	4.83	12.03	3.58	0.574	0.426
0.65	1.32	4.54	10.81	3.22	0.585	0.415
0.70	1.38	4.46	10.34	3.08	0.591	0.409
0.75	1.45	3.95	8.38	2.49	0.613	0.387
0.80	1.53	3.79	7.59	2.26	0.627	0.373
0.85	1.60	3.52	6.47	1.92	0.647	0.353
0.90	1.68	3.11	4.81	1.43	0.685	0.315
0.95	1.76	2.81	3.54	1.05	0.727	0.273
1.00	1.92	2.05	0.46	0.14	0.937	0.063

[a] x_1 is the mass fraction of acetonitrile (1) in the {acetonitrile (1) + methanol (2)} mixtures free of sulfamerazine (3).
[b] Average relative standard uncertainty in w_1 is $u_r(w_1)$ = 0.0008. Standard uncertainty in T is $u(T)$ = 0.10 K. Average relative standard uncertainty in apparent thermodynamic quantities of mixing processes are $u_r(\Delta_{mix}G°)$ = 0.022, $u_r(\Delta_{mix}H°)$ = 0.028, $u_r(\Delta_{mix}S°)$ = 0.036, $u_r(T\Delta_{mix}S°)$ = 0.036.
[c] ζ_H and ζ_{TS} are the relative contributions by enthalpy and entropy toward apparent Gibbs energy of mixing.

process performed by the solvent to contain the solute molecule is endothermic, in pure MeOH, the enthalpy of the mixture is negative, thus favoring the solution process. Regarding the entropy of the mixture, in both pure methanol and w_1 = 0.05, the values are negative, indicating a disadvantage for the mixing process. From w_1 = 0.05 to pure MeCN, the entropy of the mixture is positive, thus favoring the mixing process. In general terms, with the exception of pure MeOH (ζ_{TS} > 0.773), the enthalpy of the mixture contributes the most to the Gibbs energy value of the mixture (ζ_H > 0.544).

3.6. Enthalpy-entropy compensation analysis

The enthalpy-entropic compensation is the thermodynamic manifestation of the formation and breaking of bonds, with the hydrogen bridge being the most important bond. This analysis allows us to identify the mechanism that controls the action of the cosolvent [21–23].

Therefore, the enthalpy of the solution can be interpreted as a consequence of the changes in the intermolecular interactions between the drug and solvents through hydrogen and van der Waals bonds, being a quantitative indicator of the energetic changes that occur in the different molecular interactions. Whereas, entropy can be interpreted in terms of the rearrangements of the solute and solvent molecules in the solution process.

This analysis can be performed plotting $\Delta_{soln}H°$ vs. $\Delta_{soln}G°$, where nonlinear trends are usually obtained. From these trends, plots with negative and positive slopes indicate an entropic conduction and enthalpic condition, respectively.

Hence, according to the enthalpy-entropic compensation plot (Fig. 5), of SMR in (MeCN + MeOH) cosolvent mixtures, from pure MeOH to w_1 = 0.25, the solution process is driven by entropy. From w_1 = 0.25 to w_1 = 0.35, there is a trend with a positive slope indicating a conduction by enthalpy. Finally, from w_1 = 0.35 to pure MeCN, the process is again driven by entropy (negative slope).

3.7. Preferential solvation analysis

The preferential solvation of SMR, in (MeCN + MeOH) cosolvent mixtures is expressed in terms of the preferential solvation parameter $\delta x_{1,3}$.

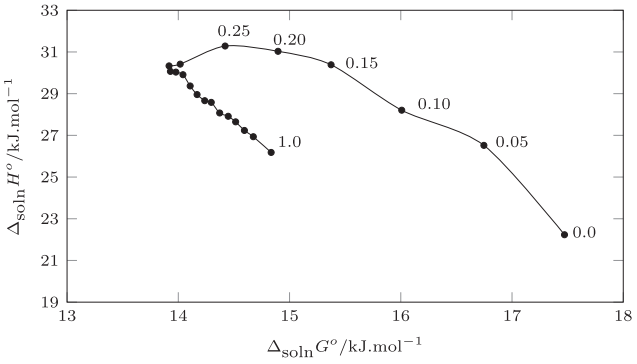

Fig. 5. Enthalpy-entropy compensation plot for the solubility of sulfamerazine (3) in {acetonitrile (1) + methanol (2)} mixtures at T_{hm} = 303.0 K. The points represent the mass fraction of acetonitrile (1) in the {acetonitrile (1) + methanol (2)} mixtures in the absence of sulfamerazine (3).

$$\delta x_{1,3} = x^L_{1,3} - x_1 = -\delta x_{2,3} \tag{10}$$

where $x^L_{1,3}$ is the local mole fraction of MeCN (1) in the molecular environment near SMR (3) and x_1 is the bulk mole fraction of MeCN (1) in the initial non-aqueous-cosolvent mixture in the absence of SMR (3). If $\delta x_{1,3}$ > 0 SMR is preferentially solvated by MeCN (1), but if this parameter is <0 SMR is preferentially solvated by MeOH (2).

The preferential solvation parameter ($\delta x_{1,3}$) can be obtained using the IKBI approach (inverse Kirkwood–Buff integrals) proposed by Ben-Naim [24,25] and reformulated by Marcus [26,27]:

$$\delta x_{1,3} = \frac{x_1 x_2 (G_{1,3} - G_{2,3})}{x_1 G_{1,3} + x_2 G_{2,3} + V_{cor}} \tag{11}$$

$$G_{1,3} = RT\kappa_T - \bar{V}_3 + x_2 \bar{V}_2 D/Q \tag{12}$$

$$G_{2,3} = RT\kappa_T - \bar{V}_3 + x_1 \bar{V}_1 D/Q \tag{13}$$

$$V_{cor} = 2522.5 \cdot \left\{ r_3 + 0.1363 \cdot \left(x_{1,3}^{L} \bar{V}_1 + x_{2,3}^{L} \bar{V}_2 \right)^{1/3} - 0.085 \right\}^3 \quad (14)$$

$$D = \left(\frac{\partial \Delta_{tr} G^{o}_{3,2\rightarrow 1+2}}{\partial x_1} \right)_{T,p} \quad (15)$$

$$Q = RT + x_1 x_2 \left(\frac{\partial^2 G^{Exc}_{1+2}}{\partial x_2^2} \right)_{T,p} \quad (16)$$

where $G_{1,3}$ and $G_{2,3}$, are the Kirkwood–Buff integrals ($cm^3 \cdot mol^{-1}$); V_{cor} is the correlation volume around the solute (SMR), wherein the preferential solvation occurs; κ_T is the isothermal compressibility of the cosolvent mixtures (MeCN + MeOH) (GPa^{-1}) calculated as $\kappa_{T1}x_1 + \kappa_{T2}x_2$; V_3, V_2, and V_1, are the molar volumes of SMR, MeOH, and MeCN, respectively ($cm^3 \cdot mol^{-1}$); D and Q ($kJ \cdot mol^{-1}$) are calculated using Eqs. (14) and (15), respectively. D is obtained from Gibbs transfer energy of SMR (Eq. (17)), which in turn is calculated from experimental solubility data.

$$\Delta_{tr} G^{o}_{3,2\rightarrow 1+2} = RT \ln \left(\frac{x_{3,2}}{x_{3,1+2}} \right) \quad (17)$$

Fig. 6 denotes the behavior of the Gibbs transfer energy, which is correlated according to Eq. (18), whose coefficients are: a = 0.03, b = –5.17, c = –22.08, d = 5.96, e = 151.71, f = –10.05, g = –299.61, h = 56.87 and i = 49.76; with r^2 = 0.9974, typical error = 0.0462, and F value = 1057.0.

$$\Delta_{tr} G^{o}_{3,2\rightarrow 1+2} = \frac{a + cx_1 + ex_1^2 + gx_1^3 + ix_1^4}{1 + bx_1 + dx_1^2 + fx_1^3 + hx_1^4} \quad (18)$$

Some data necessary for the solvation parameters calculation are taken from the literature, as follows: κ_T for MeCN (1.070 GPa^{-1}) and MeOH (1.248 GPa^{-1}) [13]; V_3 = 164.5 $cm^3 \cdot mol^{-1}$ [28]; V_1 and V_2 [16]; r_3 = 0.251 nm [28]; Q [16].

Table 6 denotes the values of the D factor, Kirkwood–Buff integrals, correlation volume, and preferential solvation parameters. $G_{1,3}$, and $G_{2,3}$ evidence negative values, indicating that SMR denotes affinity for both solvents (MeCN and MeOH).

Fig. 7 denotes the preferential solvation parameter behavior, SD and SMR. The behavior of SMT is very similar to that of SD (SD solubility data were taken from Delgado *et al.* [16]). In MeOH-rich mixtures, both SD and SMR, are preferentially solvated by MeOH. From x_1 = 0.3 to x_1 = 0.45, both sulfonamides are preferentially solvated by MeCN. However, $\delta x_{1,3}$ values are smaller than |0.01| and thus, apparently the preferential solvation is not significant with MeCN. From x_1 = 0.45 to pure MeCN, both SD and SMR, are also preferentially solvated by MeOH. However, similarly, $\delta x_{1,3}$ values are smaller than |0.01|, indicating that the preferential solvation by MeOH is not significant. This is consistent with the negative heats of the Kirkwood–Buff integrals, indicating that there is no significant preference for any solvent.

Although, in MeOH-rich mixtures, when adding MeCN the solubility of SMR increases, Fig. 7 shows a preferential solvation by MeOH, a phenomenon very similar to that happens in aqueous media [29,30]. This event possibly occurs because when adding MeCN, in principle, MeCN interacts with MeOH, destructuring the H-bonded-arrangement of MeOH, allowing a better MeOH-SMR interaction, however, in MeCN-rich mixtures, MeCN acts as an anti-solvent decreasing the SMR solubility.

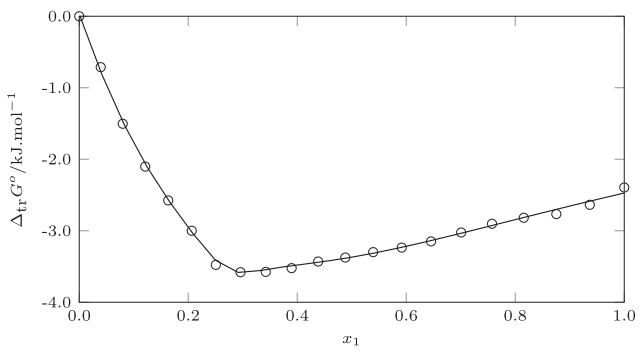

Fig. 6. Gibbs energy of transfer of sulfamerazine (3) from neat methanol (2) to {acetonitrile (1) + methanol (2)} mixtures at 298.15 K.

3.8. Solubility modeling

To identify the mathematical models that best fit the experimental data of SMR solubility in (MeCN + MeOH) solvent mixtures, nine models were evaluated (Apelblat, van't Hoff, Yaws, λh, Weibull, NRTL, Wilson, modified Wilson, and Jouyban-Acree-van't Hoff). These models calculates the solubility in binary solvents with respect to only temperature in a given solvent composition (class I models), only solvent composition at isothermal condition (class II models) and both temperature and solvent compositions (class III models). A brief mathematical description of each model is presented below.

3.8.1. Apelblat model

The semiempirical Apelblat model (Eq. (19)) relates the temperature (T/K) and solubility in mole fraction [31,32].

$$\ln x_3 = A + \frac{B}{T} + C \ln T \quad (19)$$

where x_3 is SMR solubility, T is temperature (K), A and B is the relationship between the activity coefficient and solubility in the non-ideal state, and C measures the influence of temperature on fusion enthalpy [33,34].

3.8.2. van't Hoff equation

The van't Hoff equation is also a semiempirical equation that relates solubility (x_3) and temperature (K) (Eq. (20)) [34,35]

$$\ln x_3 = A + \frac{B}{T} \quad (20)$$

where x_3 is SMR solubility and T is temperature (K). The A and B parameters are related to the enthalpy and entropy of the solution, respectively [34,36].

3.8.3. Yaws model

Yaws' model is also a semiempirical model that relates solubility with temperature according to (Eq. (21)) [37,38]:

$$\ln x_3 = A + \frac{B}{T} + \frac{C}{T^2} \quad (21)$$

where A, B, and C are fitting model parameters.

3.8.4. Buchowski–Ksiazaczak λh model

Similar to the previous models, the λh model (Eq. (22)) presents a relationship between temperature and drug solubility (x_3).

$$\ln \left[1 + \lambda \frac{(1 - x_3)}{x_3} \right] = \lambda h \left(\frac{1}{T} - \frac{1}{T_f} \right) \quad (22)$$

where T_f is the melting temperature of the drug, and λ and h are model parameters [34,39,40].

Table 6
Some properties associated to preferential solvation of sulfamerazine (3) in {acetonitrile (1) + methanol (2)} mixtures at 298.15 K.

x_1[a]	D/kJ mol^{-1}	$G_{1,3}$/cm^3 mol^{-1}	$G_{2,3}$/cm^3 mol^{-1}	V_{cor}/cm^3 mol^{-1}	100 $\delta x_{1,3}$
0.00	−21.94	−530.1	−161.4	1244	0.00
0.05	−18.04	−502.1	−184.3	1247	−1.44
0.10	−14.39	−458.3	−203.6	1252	−2.24
0.15	−11.64	−415.1	−218.9	1260	−2.47
0.20	−10.29	−390.5	−235.2	1268	−2.48
0.25	−7.49	−326.4	−232.5	1278	−1.72
0.30	0.24	−156.4	−158.7	1291	0.04
0.35	1.44	−132.9	−141.5	1301	0.17
0.40	1.06	−141.9	−144.5	1311	0.05
0.45	1.12	−142.7	−141.4	1321	−0.03
0.50	1.33	−141.1	−134.9	1331	−0.13
0.55	1.54	−140.3	−127.6	1342	−0.26
0.60	1.71	−140.7	−120.6	1352	−0.40
0.65	1.82	−142.3	−114.6	1363	−0.51
0.70	1.89	−144.8	−110.1	1374	−0.59
0.75	1.92	−147.9	−107.4	1385	−0.61
0.80	1.92	−151.3	−106.9	1396	−0.57
0.85	1.90	−154.6	−108.7	1407	−0.47
0.90	1.87	−157.6	−112.5	1418	−0.32
0.95	1.82	−160.1	−117.9	1429	−0.16
1.00	1.77	−161.8	−123.9	1440	0.00

[a] x_1 is the mole fraction of acetonitrile (1) in the {acetonitrile (1) + methanol (2)} mixtures free of sulfamerazine (3).

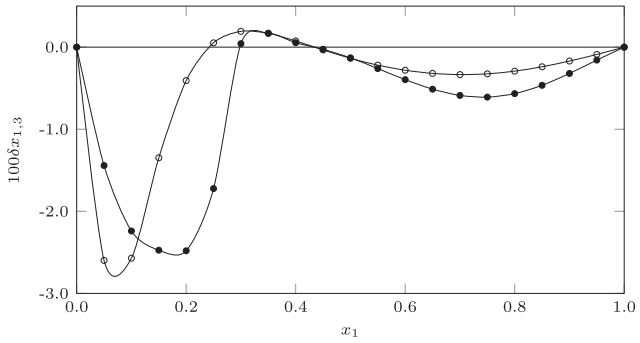

Fig. 7. Preferential solvation parameters of sulfamerazine (3, ●) and sulfadiazine (3, ○) by acetonitrile (1) in {acetonitrile (1) + methanol (2)} mixtures at 298.15 K.

3.8.5. Two-parameter Weibull function

Svärd and Rasmuson presented the importance of boundary conditions necessary to estimate solubility via extrapolation to lower or higher temperatures up to the melting point [41]. Hence, the Weibull distribution was the basis for the development of Eq. (23) [42], which defines the probability density function of a random variable [43].

$$\ln\gamma_3 = \frac{A}{T}\left[1 - e^{-\left(\frac{B}{T}+\frac{B}{T_f}\right)^C}\right] \tag{23}$$

where A and B, are the adjustable parameters of the model. However, because the model requires $C \geq 2$, this value was held constant at 2 [44].

3.8.6. Wilson model

The Wilson model expresses the activity coefficient of a multicomponent solution as [45]:

Table 7
Apelblat model parameter and corresponding MRD% for sulfamerazine in {acetonitrile (1) + methanol (2)} mixtures.

w_1	A	B	C	MRD%
0.00	112.931	−7618.228	−16.570	1.5
0.05	91.010	−7067.079	−12.996	1.2
0.10	54.727	−5610.504	−7.433	0.4
0.15	−104.862	1301.615	16.549	1.5
0.20	−183.563	4750.079	28.365	2.2
0.25	−41.925	−1589.242	7.274	1.1
0.30	38.370	−5076.528	−4.736	0.8
0.35	21.252	−4290.628	−2.187	0.9
0.40	−47.385	−1205.719	8.041	0.9
0.45	−71.064	−158.384	11.576	0.8
0.50	−116.547	1866.245	18.362	0.5
0.55	−105.124	1415.399	16.618	0.5
0.60	−126.522	2411.079	19.783	0.7
0.65	−154.395	3679.880	23.922	0.9
0.70	−151.965	3575.935	23.553	0.7
0.75	−193.090	5448.869	29.662	0.9
0.80	−256.065	8256.851	39.054	1.1
0.85	−283.546	9502.680	43.139	1.5
0.90	−380.622	13860.675	57.604	1.3
0.95	−458.368	17345.598	69.190	1.3
1.00	−736.831	29784.660	110.723	2.1
Overall MRD%				1.9

Table 8
van't Hoff model parameter and corresponding MRD% for sulfamerazine in {acetonitrile (1) + methanol (2)} mixtures.

w_1	A	B	MRD%
0.00	1.918	−2672.022	1.5
0.05	3.938	−3186.121	1.3
0.10	4.919	−3389.109	0.5
0.15	6.093	−3662.341	1.2
0.20	6.580	−3749.836	1.6
0.25	6.832	−3767.666	0.9
0.30	6.626	−3657.679	0.7
0.35	6.626	−3645.688	1.0
0.40	6.530	−3618.647	0.7
0.45	6.515	−3619.896	0.8
0.50	6.470	−3614.418	1.4
0.55	6.217	−3546.685	1.2
0.60	6.032	−3499.139	1.3
0.65	5.898	−3467.685	1.5
0.70	5.844	−3458.590	1.5
0.75	5.641	−3407.225	2.2
0.80	5.599	−3404.063	2.8
0.85	5.493	−3380.450	3.1
0.90	5.356	−3349.225	4.0
0.95	5.265	−3331.896	4.5
1.00	5.214	−3336.123	7.3
Overall MRD%			1.9

$$\ln\gamma_i = -\ln\left(\sum_{j=0}^{m} x_j\Lambda_{ij}\right) + 1 - \left(\frac{\sum_{k=0}^{m} x_k}{\sum_{j=0}^{m} x_j\Lambda_{ki}}\right) \tag{24}$$

where, Λ_{ij} is the binary interaction solvation parameter expressed as [46]:

$$\Lambda_{ij} = a_{ij} + \frac{b_{ij}}{T} \tag{25}$$

For SMR solubility (3) in {MeCN (1) + MeOH (2)} cosolvent mixtures, the Wilson model is expressed as:

$$\ln\gamma_3 = 1 - \ln(x_3 + x_2\Lambda_{32} + x_1\Lambda_{31}) - \left[\frac{x_3}{(x_3 + x_2\Lambda_{32} + x_1\Lambda_{31})} + \frac{x_2\Lambda_{23}}{(x_3\Lambda_{23} + x_2 + x_1\Lambda_{21})} + \frac{x_1\Lambda_{13}}{(x_3\Lambda_{13} + x_2\Lambda_{12} + x_1)}\right] \tag{26}$$

Table 10
λh model parameter and corresponding MRD% for sulfamerazine in {acetonitrile (1) + methanol (2)} mixtures.

w_1	λ	h	MRD%
0.00	0.031	82975.478	1.5
0.05	0.091	34432.063	1.3
0.10	0.166	20196.402	0.6
0.15	0.321	11371.330	1.1
0.20	0.442	8453.156	1.6
0.25	0.552	6802.878	0.9
0.30	0.557	6546.660	0.7
0.35	0.571	6368.884	1.0
0.40	0.546	6610.037	0.7
0.45	0.535	6738.433	0.8
0.50	0.517	6967.246	1.3
0.55	0.456	7741.287	1.1
0.60	0.415	8395.041	1.2
0.65	0.385	8960.654	1.4
0.70	0.370	9277.583	1.4
0.75	0.333	10166.609	2.1
0.80	0.320	10543.179	2.7
0.85	0.301	11143.028	3.0
0.90	0.278	11953.896	3.9
0.95	0.261	12621.745	4.4
1.00	0.245	13487.777	7.1
Overall MRD%			1.9

3.8.7. NRTL model

The NRTL model was proposed by Renon and Prausnitz in 1968 based on the concept of local composition [47,48]. For partial and complete miscible systems, the model can provide a perfect correlation of the experimental data. Hence, the NRTL model is expressed as [45,49]:

$$\ln\gamma_i = \frac{\sum_j \tau_{ji} G_{ji} x_j}{\sum_k G_{ki} x_k} + \sum_j \frac{x_j G_{ij}}{G_{ki} x_k}\left(\tau_{ij} - \frac{\sum_n x_n \tau_{nj} G_{nj}}{\sum_k G_{kj} x_k}\right) \tag{27}$$

where $G_{ij} = \exp(\alpha_{ij}.\tau_{ij})$, $\alpha_{ij} = \alpha_{jj}$, $\tau_{ii} = \tau_{jj} = 0$, and τ_{ij} is the binary interaction parameters, expressed as:

$$\tau_{ij} = \frac{g_{ij} - g_{ii}}{RT} \tag{28}$$

For SMR solubility (3) in {MeCN (1) + MeOH (2)} cosolvent mixtures, the Wilson model is expressed as:

Table 9
Yaws model and corresponding MRD% for sulfamerazine in {acetonitrile (1) + methanol (2)} mixtures.

w_1	A	B	C	MRD%
0.00	−6.285	2228.346	−730511.936	1.5
0.05	−2.521	674.226	−575729.116	1.3
0.10	1.207	−1169.339	−331310.479	0.4
0.15	14.175	−8512.549	726460.752	1.5
0.20	20.533	−12116.238	1251972.910	2.2
0.25	10.464	−5943.988	325514.265	1.1
0.30	4.328	−2280.448	−206029.834	0.8
0.35	5.467	−2960.665	−101001.137	0.9
0.40	10.466	−5981.931	354132.868	0.9
0.45	12.313	−7089.788	518192.699	0.9
0.50	15.751	−9159.178	826646.636	0.5
0.55	14.582	−8546.403	745643.215	0.5
0.60	15.950	−9429.442	884873.189	0.8
0.65	17.876	−10630.022	1068787.916	0.9
0.70	17.668	−10527.112	1054414.129	0.7
0.75	20.602	−12348.473	1333384.637	1.0
0.80	25.321	−15191.275	1757868.580	1.1
0.85	27.275	−16401.245	1942232.115	1.6
0.90	34.329	−20674.885	2585287.878	1.4
0.95	39.990	−24102.787	3100201.244	1.4
1.00	60.618	−36506.937	4955429.681	2.2
Overall MRD%				1.1

Table 11
Two-parameter Weibull model and corresponding MRD% for sulfamerazine in {acetonitrile (1) + methanol (2)} mixtures (C = 2.0).

w_1	A	B	MRD%
0.00	546.277	30573106.4	9.8
0.05	460.266	25481126.7	2.4
0.10	371.975	20238099.7	1.9
0.15	296.224	15725072.0	5.7
0.20	239.114	12397222.5	7.1
0.25	182.084	9191207.6	8.4
0.30	133.412	6551691.7	7.9
0.35	121.359	5735010.5	7.8
0.40	122.780	6115740.9	7.3
0.45	128.665	6727484.9	7.2
0.50	136.284	7024845.3	7.0
0.55	143.932	7480049.1	6.1
0.60	151.295	7837393.2	5.3
0.65	159.487	8398962.5	4.8
0.70	166.519	8803059.2	4.6
0.75	175.485	9601257.5	3.8
0.80	184.664	10379113.4	3.9
0.85	192.613	11168744.8	3.7
0.90	201.991	11918644.3	3.3
0.95	211.531	12476158.7	3.5
1.00	230.606	14416578.8	6.1
Overall MRD%			5.6

$$\ln\gamma_3 = \frac{x_2\tau_{23}G_{23}+x_1\tau_{13}G_{13}}{x_3+x_2G_{23}+x_3G_{13}} - x_3\frac{(x_2\tau_{23}G_{23}+x_1\tau_{13}G_{13})}{(x_3+x_2G_{23}+x_3G_{13})^2} + \frac{x_2G_{32}}{x_3G_{32}+x_2+x_1G_{12}}\left(\tau_{32} - \frac{x_3\tau_{32}G_{32}+x_1\tau_{12}G_{12}}{x_3G_{32}+x_2+x_1G_{12}}\right) + \frac{x_1G_{31}}{x_3G_{31}+x_2G_{21}+x_1}\left(\tau_{31} - \frac{x_3\tau_{31}G_{31}+x_2\tau_{21}G_{21}}{x_3G_{31}+x_2G_{31}+x_1}\right) \quad (29)$$

3.8.8. Modified Wilson model

Modified Wilson is a nonlinear model, representing drug solubility in binary solvents at a given temperature [50]. The model is:

$$-\ln x_{3,1+2} = 1 - w_1\frac{(1+\ln x_{3,1})}{(w_1+w_2\lambda_{12})} - w_2\frac{(1+\ln x_{3,2})}{(w_2+w_1\lambda_{21})} \quad (30)$$

where $x_{3,1+2}$, $x_{3,1}$, and $x_{1,2}$, are the solute solubility in the cosolvent mixtures and mono-solvents 1 and 2 at constant temperature, respectively; w_1 and w_2 are the mass fraction of the solute free solvents 1, 2; λ_{12} and λ_{21} are model parameters.

3.8.9. Jouyban-Acree-van't Hoff model

The Jouyban-Acree-van't Hoff model, is a logical combination of the Jouyban-Acree and the van't Hoff models to represent the effects of solvent composition and temperature effects on drug solubility [50] and represented as:

$$\ln x_{3,1+2,T} = w_1\left(A_1+\frac{B_1}{T}\right) + w_2\left(A_2+\frac{B_2}{T}\right) + \frac{w_1w_2}{T} \times \sum_0^2 (w_1-w_2)^i \quad (31)$$

where $x_{3,1+2,T}$, $x_{3,1,T}$, and $x_{1,2,T}$, are the solute solubility in the cosolvent mixtures at temperature of T, A_1, B_1, A_2 and B_2 are the van't Hoff model's constants for the mono-solvents at various temperatures taken from Table 8 and the J_i terms are the Jouyban-Acree model constants computed using linear regression of $\ln x_{3,1+2,T} - w_1\left(A_1+\frac{B_1}{T}\right) - w_2\left(A_2+\frac{B_2}{T}\right)$ vs $\frac{w_1w_2}{T}$, $\frac{w_1w_2(w_1-w_2)}{T}$, and $\frac{w_1w_2(w_1-w_2)^2}{T}$.

The parameters for each model are presented in Tables 7–14. To evaluate the applicability and precision of the used models, the relative mean deviation (MRD%) was calculated using Eq. (32).

$$\text{MRD\%} = \frac{100}{N}\sum\left(\frac{x_3^{Calc}-x_3^{Exp}}{x_3^{Exp}}\right) \quad (32)$$

where x_3^{Calc} is the solubility calculated with each one of the models, and x_3^{Exp} is the experimental solubility.

Table 12
NRTL model parameter and corresponding MRD% for sulfamerazine in {acetonitrile (1) + methanol (2)} mixtures.

T/K	τ_{12}	τ_{13}	τ_{21}	τ_{23}	τ_{31}	τ_{32}	MRD%
278.15	−3.598	−3.288	12.927	1.285	10.013	−1.288	0.3
283.15	−3.493	−3.149	12.265	1.033	9.231	−1.045	0.3
288.15	4.043	3.787	0.568	−4.753	−0.476	−14.112	6.0
293.15	−3.305	−2.896	11.148	0.809	7.980	−0.818	0.6
298.15	−3.202	−2.745	10.613	0.646	7.324	−0.651	0.7
303.15	−3.111	−2.621	10.133	0.604	6.785	−0.608	0.8
308.15	−3.044	−2.526	9.844	0.780	6.343	−0.794	0.7
313.15	−2.966	−2.431	9.487	0.784	5.933	−0.802	0.6
318.15	−2.815	−2.338	8.810	2.270	5.503	−1.824	0.2
Overall MRD%							1.1

Table 13
Wilson model parameter and corresponding MRD% for sulfamerazine in {acetonitrile (1) + methanol (2)} mixtures.

T/K	Λ_{12}	Λ_{13}	Λ_{21}	Λ_{23}	Λ_{31}	Λ_{32}	MRD%
278.15	0.0001	−0.0003	5.887	1.605	5.892	0.598	0.1
283.15	0.0002	−0.0003	5.702	1.882	5.740	0.507	0.2
288.15	−0.0001	0.0007	5.537	1.908	5.548	0.492	0.2
293.15	−0.0002	0.0008	5.364	2.039	5.397	0.457	0.3
298.15	0.0004	0.0011	5.172	1.890	5.209	0.482	0.4
303.15	0.0005	0.0013	5.011	1.896	5.054	0.474	0.5
308.15	0.0006	0.0020	4.840	1.953	4.887	0.450	0.6
313.15	0.3915	10.0449	−0.009	−10.941	−2.033	1.084	6.0
318.15	0.0013	0.0049	4.445	2.165	4.532	0.368	0.8
Overall MRD%							1.0

Table 14
Modified Wilson model parameter and corresponding MRD% for sulfamerazine in {acetonitrile (1) + methanol (2)} mixtures.

T/K	Λ_{12}	Λ_{21}	MRD%
278.15	0.593	2.397	5.2
283.15	0.634	2.419	4.6
288.15	0.647	2.547	4.7
293.15	0.665	2.595	4.4
298.15	0.711	2.617	4.1
303.15	0.723	2.696	3.9
308.15	0.658	2.977	4.1
313.15	0.656	3.099	4.3
318.15	0.555	3.607	4.6
Overall MRD%			4.4

The trained version of the Jouyban-Acree-van't Hoff model to calculate SMR solubility in MeCN + MeOH mixtures at various temperatures is:

$$\ln x_{3,1+2,T} = w_1\left(5.214 - \frac{3336.123}{T}\right) + w_2\left(1.918 - \frac{2672.022}{T}\right) + \frac{1047.285 w_1 w_2}{T} - \frac{764.659 w_1 w_2 (w_1 - w_2)^i}{T} + \frac{203.669 w_1 w_2 (w_1 - w_2)^i}{T} \quad (33)$$

which correlates the data with the MRD% of 9.0%.

According to the MRD%, SMR solubility is calculated for each model, in general, exhibits good correlation with the experimental data as MRD% is <10%. It is noteworthy that the modified Wilson model only requires two experimental data corresponding to SMR solubility data in the two mono-solvents (MeCN and MeOH).

The model with the lowest overall MRD% in class II models, is the Wilson model (MRD% = 1.0%), followed by the NRTL (MRD% = 1.1%) and modified Wilson (MRD% = 4.4%). For the class I models the Yaws model (MRD% = 1.1%) showed the best performance and followed by the van't Hoff, Apelblat, and λh models reported an MRD% of 1.9%, and Weibull model (MRD% = 5.6%). The model from class III models with the highest MRD% (9.0%) among all investigated models. It is obvious that the models in classes I and II correlate the solubility with only one independent variable, whereas the model from class III correlates with two independent

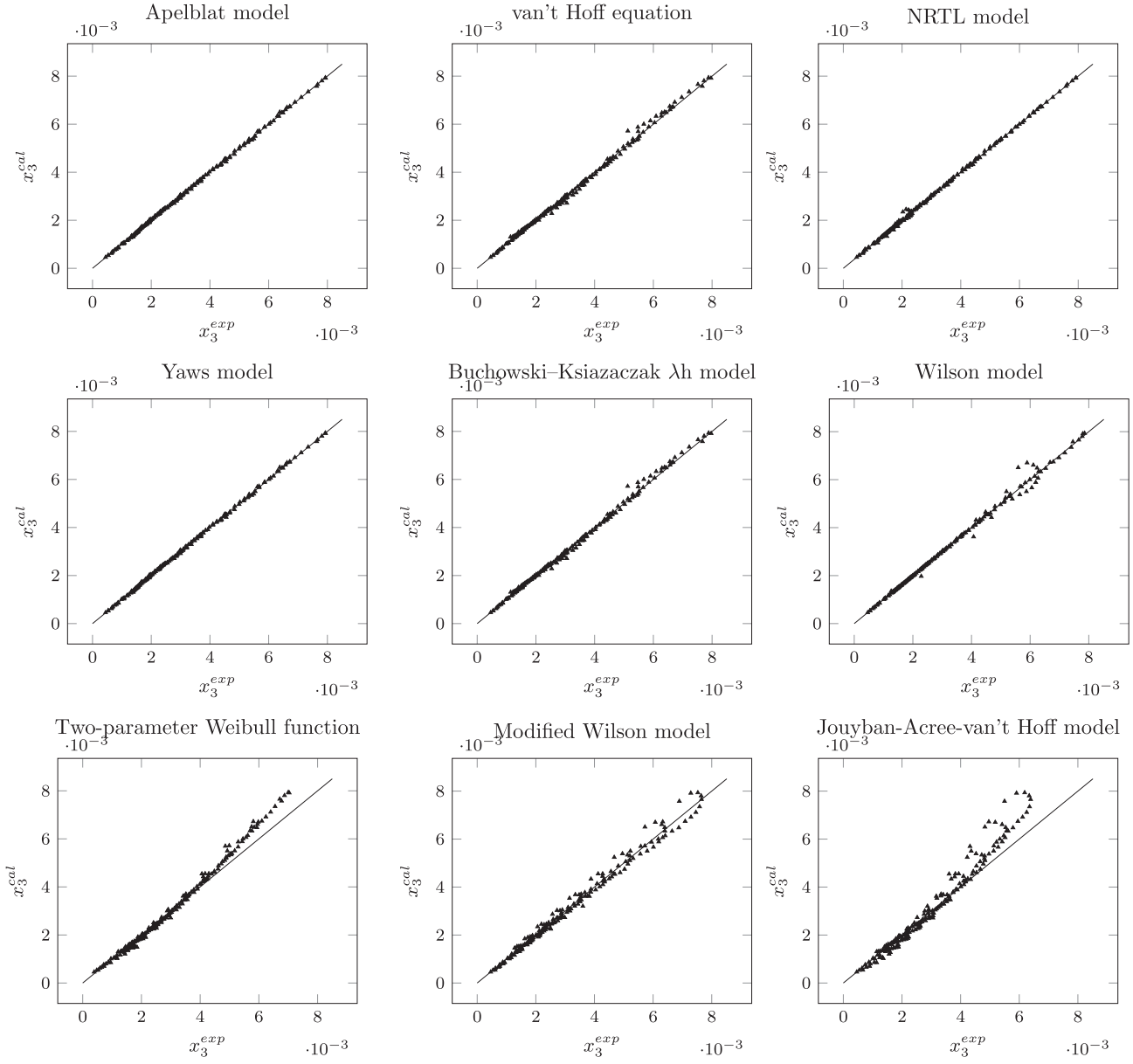

Fig. 8. Calculated solubility vs experimental solubility of sulfamerazine in acetonitrile + methanol cosolvent mixtures.

parameters and is more applicable in industrial applications where changing the solvent mixture and temperature are employed in the processes.

Finally, in Fig. 8, it can be observed that in general all the models present a good correlation with the experimental data.

4. Conclusions

SMR solubility is an endothermic process dependent on cosolvent system polarity. Gibbs energy is positive in all cases, as is the enthalpy and entropy of the solution, indicating an entropic favoring. Regarding the enthalpy-entropic compensation analysis, entropy drives the process in most cosolvent mixtures, except for some intermediate mixtures. SMR is preferentially solvated using MeOH in MeOH-rich mixtures. In MeCN-intermediate and rich mixtures, the solvation parameter is <0.01; therefore, it is not possible to identify with certainty the solvent that preferentially solvates SMR. Finally, the models developed in this study proved as a useful tool for calculating SMR solubility in (MeCN + MeOH) solvent mixtures.

CRediT authorship contribution statement

Rossember E. Cárdenas: Software, Validation. **Claudia Patricia Ortiz:** Data curation, Writing – original draft. **William E. Acree:** Software, Validation. **Abolghasem Jouyban:** . **Fleming Martínez:** Conceptualization, Methodology. **Daniel Ricardo Delgado:** Writing – review & editing.

Declaration of Competing Interest

The authors declare that they have no known competing financial interests or personal relationships that could have appeared to influence the work reported in this paper.

Acknowledgments

We thank the National Directorate of Research and National Committee for Research Development of the Universidad Cooperativa de Colombia, for the financial support of the Project "Análisis matemático y termodinámico de la solubilidad algunas sustancias antimicrobianas de uso industrial en mezclas cosolventes" with code INV2976. We also thank the Universidad Cooperativa de Colombia, Sede Neiva, for facilitating the laboratories and equipments used.

References

[1] S. Padberg, Anti-infective Agents, in: Drugs Dur. Pregnancy Lact. Treat. Options Risk Assess, third ed., Elsevier Inc., 2015, pp. 115–176. https://doi.org/10.1016/B978-0-12-408078-2.00007-X.
[2] B.T. Lunestad, O. Samuelsen, Veterinary drug use in aquaculture, in: Improv. Farmed Fish Qual. Saf., Elsevier Inc., 2008, pp. 97–127. https://doi.org/10.1533/9781845694920.1.97.
[3] M.W. Griffiths, M. Walkling-Ribeiro, Microbial decontamination of milk and dairy products, in: Microb. Decontam. Food Ind. Nov. Methods Appl., Elsevier Ltd., 2012, pp. 190–238. https://doi.org/10.1533/9780857095756.1.190.
[4] Y. Escobedo, A. Espinosa, M. del R. Roble, M. del C. Bermúdez, Transformación y acumulación de sulfametazina en porcinos alimentados con una dieta medicada, Rev. Mex. Cienc. Farm. 38 (2007) 5–13.
[5] A. Martin, P. Bustamante, Physical Pharmacy: Physical Chemical Principles in the Pharmaceutical Sciences, fourth ed., Lippincott Williams & Wilking, Philadelphia, 1933.
[6] Daniel R. Delgado, Fleming Martínez, Solution thermodynamics and preferential solvation of sulfamerazine in methanol + water mixtures, J. Solution Chem. 44 (2) (2015) 360–377, https://doi.org/10.1007/s10953-015-0317-1.
[7] D.R. Delgado, F. Martínez, Solubility and solution thermodynamics of sulfamerazine and sulfamethazine in some ethanol+water mixtures, Fluid Phase Equilib. 360 (2013) 88–96, https://doi.org/10.1016/j.fluid.2013.09.018.
[8] D.R. Delgado, F. Martínez, Solubility and solution thermodynamics of some sulfonamides in 1-propanol + water mixtures, J. Solut. Chem. 43 (2014) 836–852, https://doi.org/10.1007/s10953-014-0169-0.
[9] Joaquín H. Blanco-Márquez, Claudia P. Ortiz, Nestor Enrique Cerquera, Fleming Martínez, Abolghasem Jouyban, Daniel Ricardo Delgado, Thermodynamic analysis of the solubility and preferential solvation of sulfamerazine in (acetonitrile + water) cosolvent mixtures at different temperatures, J. Mol. Liq. 293 (2019) 111507, https://doi.org/10.1016/j.molliq.2019.111507.
[10] María del Mar Muñoz, Daniel R. Delgado, María Ángeles Peña, Abolghasem Jouyban, Fleming Martínez, Solubility and preferential solvation of sulfadiazine, sulfamerazine and sulfamethazine in propylene glycol + water mixtures at 298.15 K, J. Mol. Liq. 204 (2015) 132–136, https://doi.org/10.1016/j.molliq.2015.01.047.
[11] C. Aloisio, A.G. de Oliveira, M. Longhi, Solubility and release modulation effect of sulfamerazine ternary complexes with cyclodextrins and meglumine, J. Pharm. Biomed. Anal. 100 (2014) 64–73, https://doi.org/10.1016/j.jpba.2014.07.008.
[12] J.A. Riddick, W.B. Bunger, T. Sakano, Organic Solvents: Physical Properties and Methods of Purification, fourth ed., Wiley, New York, 1986.
[13] Y. Marcus, The Properties of Solvents, John Wiley & Sons Ltd, New York, 1999.
[14] F.T. Tewes, F. Boury, J.P. Benoit, Biodegradable Microspheres: Advances in Production Technology, in: Microencapsulation, second ed., CRC Press, New York (NY), 2020, pp. 27–79. https://doi.org/10.1201/9781420027990-5.
[15] Q. Zhang, Y. Yang, C. Cao, L. Cheng, Y. Shi, W. Yang, Y. Hu, Thermodynamic models for determination of the solubility of dibenzothiophene in (methanol + acetonitrile) binary solvent mixtures, J. Chem. Thermodyn. 80 (2015) 7–12, https://doi.org/10.1016/j.jct.2014.08.012.
[16] Daniel Ricardo Delgado, Otto Bahamón-Hernandez, Nestor Enrique Cerquera, Claudia Patricia Ortiz, Fleming Martínez, Elaheh Rahimpour, Abolghasem Jouyban, William E. Acree, Solubility of sulfadiazine in (acetonitrile + methanol) mixtures: determination, correlation, dissolution thermodynamics and preferential solvation, J. Mol. Liq. 322 (2021) 114979, https://doi.org/10.1016/j.molliq.2020.114979.
[17] Daniel Ricardo Delgado, Diego Iván Caviedes-Rubio, Claudia Patricia Ortiz, Yarly Lizeth Parra-Pava, María Ángeles Peña, Abolghasem Jouyban, Seyyedeh Narjes Mirheydari, Fleming Martínez, William E. Acree, Solubility of sulphadiazine in (acetonitrile + water) mixtures: measurement, correlation, thermodynamics and preferential solvation, Phys. Chem. Liq. 58 (3) (2020) 381–396, https://doi.org/10.1080/00319104.2019.1594227.
[18] A. Barton, CRC Handbook of Solubility Parameters and Other Cohesion Parameters, second ed., CRC Press LLC, Boca Raton (FL), 1991.
[19] Martha Sofía Vargas-Santana, Ana María Cruz-González, Claudia Patricia Ortiz, Daniel Ricardo Delgado, Fleming Martínez, María Ángeles Peña, William E. Acree, Abolghasem Jouyban, Solubility of sulfamerazine in (ethylene glycol + water) mixtures: measurement, correlation, dissolution thermodynamics and preferential solvation, J. Mol. Liq. 337 (2021) 116330, https://doi.org/10.1016/j.molliq.2021.116330.
[20] W.C. Pierce, D.P. MacMillan, X-ray studies on liquids: the inner peak for alcohols and acids, J. Am. Chem. Soc. 60 (4) (1938) 779–783, https://doi.org/10.1021/ja01271a013.
[21] Fleming Martínez, M. Ángeles Peña, Pilar Bustamante, Thermodynamic analysis and enthalpy-entropy compensation for the solubility of indomethacin in aqueous and non-aqueous mixtures, Fluid Ph. Equilibria. 308 (1-2) (2011) 98–106, https://doi.org/10.1016/j.fluid.2011.06.016.
[22] P. Bustamante, B. Escalera, Enthalpy and entropy contributions to the solubility of sulphamethoxypyridazine in solvent mixtures showing two solubility maxima, J. Pharm. Pharmacol. 47 (1995) 550–555, https://doi.org/10.1111/j.2042-7158.1995.tb06712.x.
[23] Ernest Grunwald, Colin Steel, Solvent reorganization and thermodynamic enthalpy—entropy compensation, J. Am. Chem. Soc. 117 (21) (1995) 5687–5692, https://doi.org/10.1021/ja00126a009.
[24] A. Ben-Naim, Theory of preferential solvation of nonelectrolytes, Cell Biophys. 12 (1) (1988) 255–269, https://doi.org/10.1007/BF02918361.
[25] A. Ben-Naim, Preferential solvation in two- and in three-component systems, Pure Appl. Chern. 62 (1990) 25–34.
[26] Yizhak Marcus, On the preferential solvation of drugs and PAHs in binary solvent mixtures, J. Mol. Liq. 140 (1-3) (2008) 61–67, https://doi.org/10.1016/j.molliq.2008.01.005.
[27] Y. Marcus, Solvent Mixtures: Properties and Selective Solvation, first ed., Marcel Dekker Inc, New York, 2002.
[28] D.R. Delgado, F. Martínez, Preferential solvation of sulfadiazine, sulfamerazine and sulfamethazine in ethanol + water solvent mixtures according to the IKBI method, J. Mol. Liq. 193 (2014) 152–159, https://doi.org/10.1016/j.molliq.2013.12.021.
[29] Daniel R. Delgado, Abolghasem Jouyban, Fleming Martínez, Solubility and preferential solvation of meloxicam in methanol + water mixtures at 298.15 K, J. Mol. Liq. 197 (2014) 368–373, https://doi.org/10.1016/j.molliq.2014.06.006.
[30] María Ángeles Peña, Daniel Ricardo Delgado, Fleming Martínez, Preferential solvation of some n-alkyl p-substituted benzoates in propylene glycol + water cosolvent mixtures, Phys. Chem. Liq. 53 (4) (2015) 455–466, https://doi.org/10.1080/00319104.2015.1006221.
[31] Alexander Apelblat, Emanuel Manzurola, Solubilities of o-acetylsalicylic, 4-aminosalicylic, 3,5-dinitrosalicylic, and p-toluic acid, and magnesium-DL-aspartate in water from T = (278 to 348) K, J. Chem. Thermodyn. 31 (1) (1999) 85–91, https://doi.org/10.1006/jcht.1998.0424.

[32] Guangyi Zhou, Baohua Wang, Lei Ding, Jiejie Dong, Fang Wang, Chao Feng, Measurement and correlation of the solubility of Lidocaine in eight pure and mixed solvents at temperatures from (292.15 to 332.15) K, J. Mol. Liq. 242 (2017) 168–174, https://doi.org/10.1016/j.molliq.2017.06.110.
[33] Shuang Jiang, Yujia Qin, Songgu Wu, Shijie Xu, Kangli Li, Peng Yang, Kaifei Zhao, Lanlan Lin, Junbo Gong, Solubility correlation and thermodynamic analysis of sorafenib free base and sorafenib tosylate in monosolvents and binary solvent mixtures, J. Chem. Eng. Data 62 (1) (2017) 259–267, https://doi.org/10.1021/acs.jced.6b0063010.1021/acs.jced.6b00630.s001.
[34] R.E. Cardenas, L.E. Tinoco, D.M. Galindres, A. Beltrán, C.D. Oviedo, J. Osorio, Prediction of sulfadiazine solubility in some cosolvent mixtures using non-ideal solution models, Rev. Colomb. Cienc. Quím. Farm. 49 (2020) 822–842.
[35] D.J.W. Grant, M. Mehdizadeh, A.H.-L. Chow, J.E. Fairbrother, Non-linear van't Hoff solubility-temperature plots and their pharmaceutical interpretation, Int. J. Pharm. 18 (1-2) (1984) 25–38, https://doi.org/10.1016/0378-5173(84)90104-2.
[36] Edgar A. Ahumada, Daniel R. Delgado, Fleming Martínez, Solution thermodynamics of acetaminophen in some PEG 400+water mixtures, Fluid Phase Equilib. 332 (2012) 120–127, https://doi.org/10.1016/j.fluid.2012.07.004.
[37] Q. Jia, D. Lei, S. Zhang, J. Zhang, N. Liu, K. Kou, Solubility measurement and correlation for HNIW·TNT co-crystal in nine pure solvents from T = (283.15 to 318.15) K, J. Mol. Liq. (2020) 114592, https://doi.org/10.1016/j.molliq.2020.114592.
[38] L.E. Tinoco, D.M. Galindres, J. Osorio, R.E. Cárdenas, Prediction of sulfamerazine and sulfamethazine solubility in some cosolvent mixtures using non-ideal solution models, Rev. Colomb. Cienc. Quím. Farm. 50 (2021) 292–313. https://doi.org/10.15446/rcciquifa.v50n1.95463.
[39] Andrzej Ksiazczak, Jerzy Jan Kosinski, Vapour pressure of binary, three-phase (S-L-V) systems and solubility, Fluid Phase Equilib. 44 (2) (1988) 211–236, https://doi.org/10.1016/0378-3812(88)80112-2.
[40] A. Ksiazczak, K. Moorthi, I. Nagata, Solid-solid transition and solubility of even n-alkanes, Fluid Phase Equilib. 95 (1994) 15–29, https://doi.org/10.1016/0378-3812(94)80058-8.
[41] M. Svärd, Å.C. Rasmuson, (Solid + liquid) solubility of organic compounds in organic solvents – correlation and extrapolation, J. Chem. Thermodyn. 76 (2014) 124–133, https://doi.org/10.1016/j.jct.2014.03.013.
[42] W. Weibull, S. Sweden, A statistical distribution function of Wide applicability, JAM 18 (1951) 293–297.
[43] S.H. Neau, S.V. Bhandarkar, E.W. Hellmuth, Differential molar heat capacities to test ideal solubility estimations, Pharm. Res. 14 (1997) 601–605, https://doi.org/10.1023/A:1012148910975.
[44] Piotr Cysewski, Tomasz Jeliński, Dominika Procek, Aleksandra Dratwa, Solubility of Sulfanilamide and Sulfacetamide in neat solvents: Measurements and interpretation using theoretical predictive models, first principle approach and artificial neural networks, Fluid Phase Equilib. 529 (2021) 112883, https://doi.org/10.1016/j.fluid.2020.112883.
[45] S.N. Mirheydari, M. Barzegar-Jalali, W.E. Acree, H. Shekaari, A. Shayanfar, A. Jouyban, Comparison of the Models for Correlation of Drug Solubility in Ethanol + Water Binary Mixtures, J. Solut. Chem. 48 (2019) 1079–1104, https://doi.org/10.1007/s10953-019-00897-9.
[46] A. Mehrdad, A.H. Miri, Aqueous solubility of acetaminophen in the presence of 1-hexyl-3-methyl imidazolium bromide, ionic liquid as co-solvent, Fluid Phase Equilib. 425 (2016) 51–56, https://doi.org/10.1016/j.fluid.2016.05.012.
[47] R.V. Orye, J.M. Prausimitz, Multicomponent equilibria: With the wilson equation, Ind. Eng. Chem. 57 (1965) 18–26, https://doi.org/10.1021/ie50665a005.
[48] J.M. Prausnitz, Termodinamica Molecular de los Equilibrios de Fases, third ed., Prentice Hall, Madrid, 2000.
[49] Denis S. Abrams, John M. Prausnitz, Statistical thermodynamics of liquid mixtures: a new expression for the excess Gibbs energy of partly or completely miscible systems, AIChE J. 21 (1) (1975) 116–128, https://doi.org/10.1002/(ISSN)1547-590510.1002/aic.v21:110.1002/aic.690210115.
[50] A. Jouyban-Gharamaleki, The modified Wilson model and predicting drug solubility in water- cosolvent mixtures, Chem. Pharm. Bull. 46 (6) (1998) 1058–1061, https://doi.org/10.1248/cpb.46.1058.